Biosensors and Bioelectronics 55 (2014) 209–215

Contents lists available at ScienceDirect

Biosensors and Bioelectronics

journal homepage: www.elsevier.com/locate/bios

Quantum dot-based immunoassay enhanced by high-density vertical ZnO nanowire array

Jung Kim [a,1], Seyong Kwon [b,1], Je-Kyun Park [b,c,*], Inkyu Park [a,c,**]

[a] Department of Mechanical Engineering, Korea Advanced Institute of Science and Technology (KAIST), 291 Daehak-ro, Yuseong-gu, Daejeon 305-701, Republic of Korea

[b] Department of Bio and Brain Engineering, Korea Advanced Institute of Science and Technology (KAIST), 291 Daehak-ro, Yuseong-gu, Daejeon 305-701, Republic of Korea

[c] KAIST Institute for the NanoCentury, 291 Daehak-ro, Yuseong-gu, Daejeon 305-701, Republic of Korea

ARTICLE INFO

Article history:
Received 11 September 2013
Received in revised form
21 November 2013
Accepted 2 December 2013
Available online 10 December 2013

Keywords:
Quantum dot
ZnO nanowire array
Immunoassay
Fluorescence resonance energy transfer
Carcinoembryonic antigen
Biosensing

ABSTRACT

In this paper, we report an efficient and high-performance immunoassay platform by combining high-density vertical ZnO nanowire array with photostable quantum dot (QD) labeling. The ZnO nanowire array provides a large surface area for the immobilization of biomolecules, which makes it an efficient substrate for the immunoreaction of biomolecules. When a sandwich immunoassay with QD label was conducted on various substrates, the ZnO nanowire substrate showed stronger fluorescence signal than ZnO thin film and bare glass substrates by 3.8 and 8.5 times, respectively. We found that the fluorescence resonance energy transfer (FRET) from QD to ZnO nanowire could be suppressed by extending their distance with multilayer biotin–streptavidin complex. In addition, we demonstrated the QD-based immunoassay of carcinoembryonic antigen (CEA) on a ZnO nanowire substrate, showing an excellent immunoassay performance with a very low detection limit (0.001 ng/mL) and a large detection range up to 100 ng/mL.

1. Introduction

In recent years, several types of nanomaterials, including nanoparticles, nanowires, and nanotubes, have been developed by exploiting their unique physical, chemical, optical and electrical properties and versatile applicability to various technological fields. Among these nanomaterials, nanowires can be defined as one-dimensional nanostructures with diameters of tens to hundreds nanometers and no length limit. They have been used in numerous applications, including gas sensing (Medintz et al., 2003), photonic sensing (Peng et al., 2012) and biomolecule sensing (Zheng et al., 2005). In the biosensing applications, large surface area of nanowire provides abundant reaction sites for biomolecule binding, resulting in enhanced sensing signals.

As one of the most useful nanowires, ZnO nanowires have received a great attention due to their well-known synthesis methods, unique optical and electrical characteristics, and easy surface modification process (Wang, 2009). Many attempts have been tried to apply ZnO nanowires synthesized by chemical vapor deposition (CVD) process as a substrate for biomolecule detection with enhanced fluorescence signals due to large surface reaction area (Dorfman et al., 2006a, 2006b). A nanostructured ZnO substrate has also shown improvement of fluorescence signal in immunoassay (Hu et al., 2013).

Quantum dot (QD) nanoparticles are semiconducting particles whose excitons are confined in all three spatial dimensions. They exhibit superior optical properties such as tunable emission color by dimensional change, strong brightness and high photostability, making them as ideal labeling materials in various biological assays. Therefore, QDs have been utilized for various biological and clinical studies such as biomolecule detection in live/fixed cells and tissues (Liu et al., 2010b; Tak et al., 2012; Zrazhevskiy and Gao, 2013), in-vivo tracking of biomolecules (He et al., 2011; Liu et al., 2010a), and substrate-based immunoassay (Hu et al., 2010).

In this work, we propose a QD-based immunoassay platform using a high-density vertical ZnO nanowire array on glass substrate (hereafter, ZnO nanowire substrate) which provides a large surface area with abundant binding sites for biomolecules as compared to the conventional glass-based immunoassay substrates. Here, QDs were exploited as a labeling material for achieving highly sensitive bioassay by using their strong optical emission and photostability.

* Corresponding author at: Department of Bio and Brain Engineering, Korea Advanced Institute of Science and Technology (KAIST), 291 Daehak-ro, Yuseong-gu, Daejeon 305-701, Republic of Korea. Tel.: +82 42 350 4315; fax: +82 42 350 4310.

** Corresponding author at: Department of Mechanical Engineering, Korea Advanced Institute of Science and Technology (KAIST), 291 Daehak-ro, Yuseong-gu, Daejeon 305-701, Republic of Korea. Tel./fax.: +82 42 350 3240.

E-mail addresses: jekyun@kaist.ac.kr (J.-K. Park), inkyu@kaist.ac.kr (I. Park).

[1] The first two authors contributed equally to this work.

0956-5663/$ - see front matter © 2013 Elsevier B.V. All rights reserved.
http://dx.doi.org/10.1016/j.bios.2013.12.007

Interestingly, we found that fluorescence resonance energy transfer (FRET) occurs between ZnO nanowires and QDs when they are in a direct contact, which hinders multi-color, high-sensitivity immunoassay. To overcome this undesired FRET effect, we have implemented an intermediate nanostructure between QDs and ZnO nanowires by the formation of multi-layer biotin–streptavidin complex to maintain intrinsic optical properties of QDs on the ZnO nanowires. Excellent immunoassay performance of biomolecules with our novel immunoassay platform was demonstrated by showing the detection of carcinoembryonic antigen (CEA) with low detection limit and large detection range.

2. Material and methods

2.1. Chemicals and reagents

ZnO nanowires were fabricated by hydrothermal synthesis method (Greene et al., 2006). ZnO nanowire precursor solution was prepared with zinc nitrate hexahydrate ($Zn(NO_3)_2{\bullet}6H_2O$, 98%; Sigma-Aldrich), hexamethylene tetramine (HMTA, $C_6H_{12}N_4$, 99+%; Sigma-Aldrich) and polyethylenimine (PEI, $(C_2H_5N)_n$, Sigma-Aldrich) in deionized (DI) water. To attach biomolecules on the ZnO nanowires, the nanowire surface was first modified with 3-aminopropyltrietoxysilane (3-APTES, Sigma-Aldrich) and glutaraldehyde (Sigma-Aldrich) (Wang et al., 2009). Then, streptavidin (Sigma-Aldrich) and biotin (Sigma-Aldrich) were used for the formation of anti-FRET layers, which lower the FRET efficiency between ZnO nanowires and QDs. To capture carcinoembryonic antigen (CEA), monoclonal CEA antibodies (Abs) (Abcam) were immobilized to the anti-FRET layer covered on the ZnO nanowire surface. CEA protein (Abcam), polyclonal CEA Ab (Abcam), and QD605/525 conjugated secondary Abs (Invitrogen) were linked together for the detection of CEA protein.

2.2. Fabrication of ZnO nanowire-based substrates

A ZnO seed layer pattern for the synthesis of ZnO nanowire arrays was fabricated by photolithography, sputtering of ZnO thin film, and lift-off process. Square patterns (area of individual cell = 3×3 mm^2) were fabricated by photolithography with AZ9260 photoresist on a clean glass substrate. Cr layer (30 nm) was deposited by electron beam evaporation to visually distinguish the nanowire synthesis area and to enhance the adhesion of ZnO thin film seed layer on the glass substrate. ZnO thin film was coated by using RF sputtering (150 W, 3 min). Afterwards, ZnO nanowires were synthesized by immersing the glass substrate with ZnO thin film seed layer patterns in a precursor solution heated at 95 °C for 2.5 h.

Subsequently, the surface of ZnO nanowires was chemically modified for immunoassay. After washing the ZnO nanowire-grown glass substrate with DI water and drying with filtered air, it was treated with an oxygen plasma (power = 75 W) for 30 s in order to remove remaining PEI on the surface of ZnO nanowires. Then, the substrate was silanized by immersing in ethanol-based 3-APTES solution (volume/volume concentration = 4/100) at room temperature for 4 h, followed by washing with ethanol and DI water and air-blow dry. Finally, aldehyde group was attached by immersing the substrate in phosphate buffered saline (PBS) buffer solution with 2% glutaraldehyde at 4 °C overnight, followed by rinsing with DI water and air-blow dry. The surface functionalization of glass substrate with ZnO thin film (hereafter, ZnO thin film substrate) and bare glass substrate (hereafter, glass substrate) were also conducted by the same procedure.

2.3. Immunoassay design

As mentioned above, FRET occurs between QDs and ZnO nanowires due to the energy transfer from the QD to ZnO nanowire (Fig. 1a).

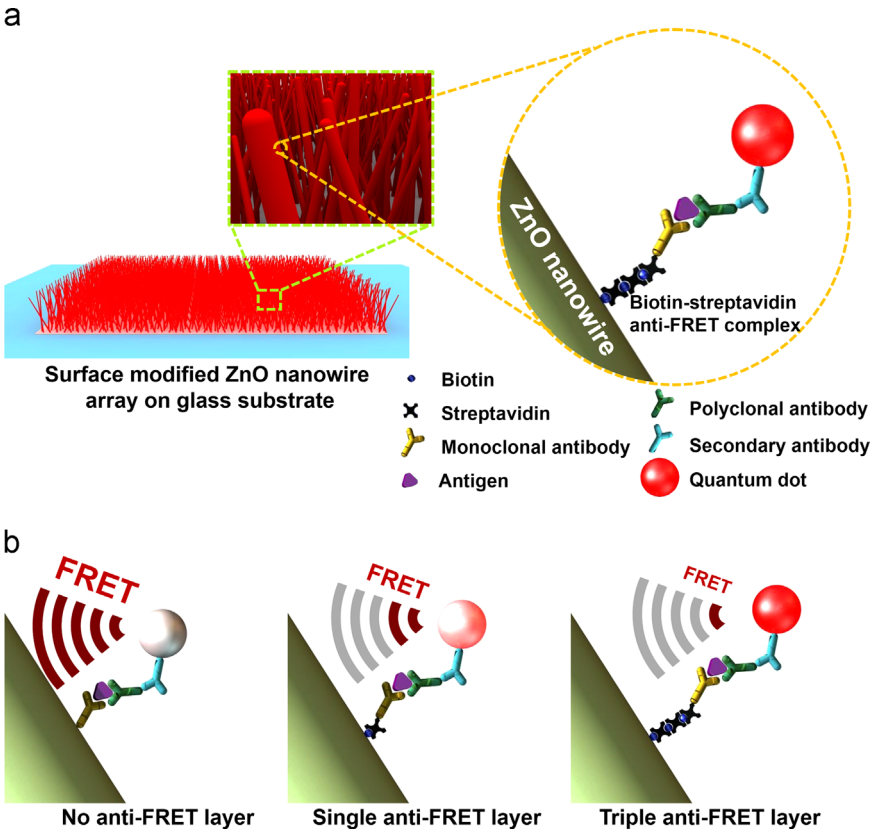

Fig. 1. Schematic of (a) QD labeled sandwich immunoreaction on the substrate with a high density vertical array of ZnO nanowires and (b) anti-FRET effect of multi-layer biotin–streptavidin conjugates by applying 0, 1 and 3 anti-FRET biotin–streptavidin complex layers.

When the QD (donor) is excited by an incident light, the excited state energy can be transferred to the ZnO nanowire (acceptor) when they are close enough (Medintz et al., 2003). In order to prevent the FRET effect and to maintain the fluorescence of QDs, aldehyde-modified ZnO nanowire substrate was coated with multiple layers of biotin–streptavidin (Fig. 1b). Briefly, 20 μL solution of biotin droplet (100 μg/mL biotin in pH 7.4 PBS) was applied on the ZnO nanowire substrate and incubated for 10 min in room temperature and washed with Tris-buffered saline plus tween 20 (TBS–T). Afterwards, 20 μL of streptavidin solution (100 μg/mL streptavidin in pH 7.4 PBS) was applied on the ZnO nanowire substrate where biotin was immobilized and incubated by the same procedure as the biotin solution. This process was repeated to form desired number of biotin–streptavidin complex layers. After obtaining desired number of biotin–streptavidin conjugate layers on the ZnO nanowires, biotin was attached at the terminal for capturing the streptavidin-conjugated monoclonal Abs. For immunoreaction, a small volume (20 μL) of analyte (i.e., CEA) solution was dropped on the immunoassay substrate, followed by incubation at a room temperature (25 °C) for 1 h. Afterwards, 20 μL of polyclonal Ab solution and 20 μL QD-labeled secondary Ab solution were sequentially dropped onto the substrate and incubated for 1 h, respectively. The fluorescence images were attained by using fluorescence microscope (IX72; Olympus) with a spectrometer (QE65000; Ocean Optics) and a charge-coupled device (CCD). A long pass filter ($\lambda > 420$ nm) was used for receiving both QD525 and QD605, while band-pass filters were used for receiving individual signals of QD525 and QD605. After the photospectra measurement, the signals from the substrate was subtracted to eliminate the auto-fluorescence of the substrate as the background noise.

3. Results and discussion

3.1. Substrate formation of ZnO nanowire-based immunoassay

Fig. 2 shows the scanning electron microscope (SEM) and transmission electron microscope (TEM) images of ZnO nanowires before and after the immunoreaction. Synthesized ZnO nanowires

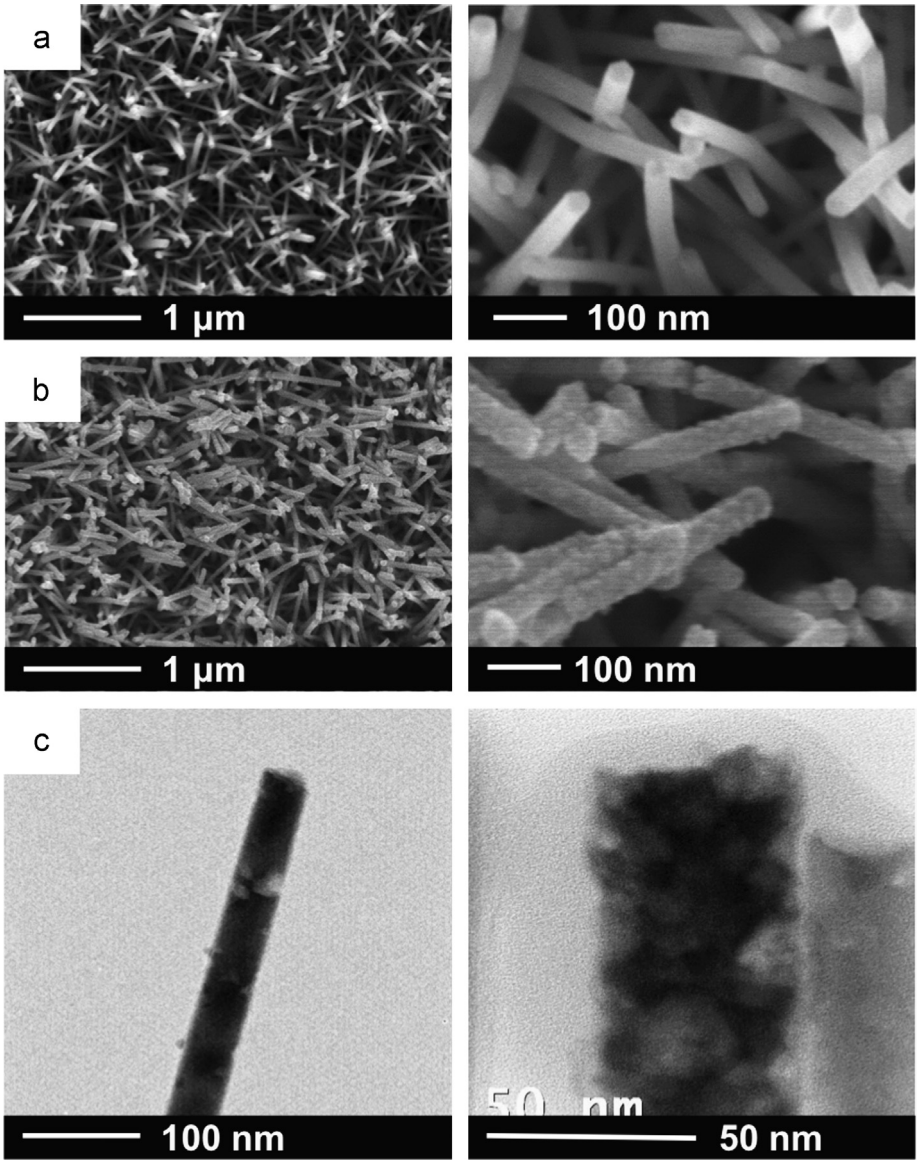

Fig. 2. (a) SEM image of ZnO nanowires before the immunoreaction with carcinoembryonic antigen (CEA). The average diameter of ZnO nanowire is ~30 nm and the average length is 2–3 μm. (b) SEM image of ZnO nanowire with immunoreaction complexes after the sandwich immunoreaction with CEA. (c) TEM images of ZnO nanowire after the sandwich immunoreaction with CEA.

have an average diameter of ~30 nm and average length of 2–3 μm as shown in Fig. 2a. After the immunoreaction, particulate structures were attached on the surface of ZnO nanowires as shown in Fig. 2b. These particulate structures were uniformly coated throughout the entire ZnO nanowire substrate. By observing higher magnification image in TEM, the diameters of individual particles were measured to be in the range of 5–15 nm (Fig. 2c). Although the composition of these particles could not be quantified due to the weak signal of energy dispersive spectrometer (EDS) analysis, we assume that these particulate structures are complex of streptavidin–biotin conjugates, monoclonal Ab, CEA, polyclonal Ab, secondary Ab, and QD. The strong Cd peaks in the x-ray photoelectron spectroscopy (XPS) analysis (See Fig. S5) on this sample confirmed the existence of CdSe quantum dots.

3.2. Effect of number of biotin–streptavidin complex

While applying QDs on the ZnO nanowire surface without biotin–streptavidin layers, we found that QD's fluorescence intensity was very weak after the immunoreaction (Fig. 3a). In addition, the emission from the substrate showed a dark yellowish color despite the emission peak of QDs at λ=605 nm (red color). This result reflects that FRET phenomenon occurred from the QDs to the ZnO nanowires after the formation of immunocomplex (monoclonal Ab–analyte–polyclonal Ab–QD labeled secondary Ab), suppressing the light emission from the QD (See Figs. S1 and S2). This FRET phenomenon has been reported by several researchers in different fields, including QD sensitized solar cells (Chang et al., 2011; Chen et al., 2010; Leschkies et al., 2007). The band gap energies of CdSe QD and ZnO nanowire are ~2 eV and ~3.3 eV, respectively. When the QD immobilized ZnO nanowire is excited by the light source of fluorescence lamp, the excited electrons of QD is transferred from the conduction band of QD to the conduction band of ZnO nanowire.

Therefore, to utilize the superior fluorescence properties of QDs in detecting CEA antigen by labeling with QDs, the FRET phenomenon should be suppressed. In our work, this was accomplished by employing an intermediate nanostructure based on biotin–streptavidin complex for the elongation of the distance between QDs and ZnO nanowires. The fluorescence energy transfer between the nanomaterials is inversely proportional to their distance (Kumar, 2007). The energy transfer efficiency can be described by the following equation:

$$\text{Efficiency} = \frac{1}{\{1+(R/R_0)^6\}} \quad (1)$$

where R is the distance between the energy donor and acceptor and R_0 is the distance at which 50% of energy transfer occurs.

To quantify the effect of number of biotin–streptavidin complexes on the FRET phenomenon, we examined the fluorescence intensity of QDs for 0, 1, 2 and 3 layers of biotin–streptavidin complex after the incubation of capture Ab, analyte, detection Ab, and QD labeled secondary Ab (Fig. 3, parts b and c). When a single layer of biotin–streptavidin complex was formed, the QD fluorescence intensity was increased by ~8.3 times higher than that for no biotin–streptavidin layer on the surface of ZnO nanowire. When dual and triple layers of biotin–streptavidin complexes were covered the surface of ZnO nanowires, the fluorescence intensity was increased by ~10.6 and ~12.5 times higher than that for no biotin–streptavidin layer, respectively. This result confirms that biotin–streptavidin layers can reduce the FRET efficiency between QD and ZnO nanowire.

When we utilized different type of QD (QD525, λpeak=525 nm), the same yellowish color could be observed due to the weakening of QD fluorescence by FRET and autofluorescence from ZnO nanowires (Fig. S3). However, when triple layers of biotin–streptavidin were formed on the surface of ZnO nanowires, intrinsic colors of both QD525 and QD605 could be observed by sandwich immunoreaction of CEA (Fig. 4a and b). This result demonstrates the potential capability of multiplexed immunodetection of several analytes with different QDs on the same location of nanowire substrates by using our platform. We have also characterized the selectivity of our

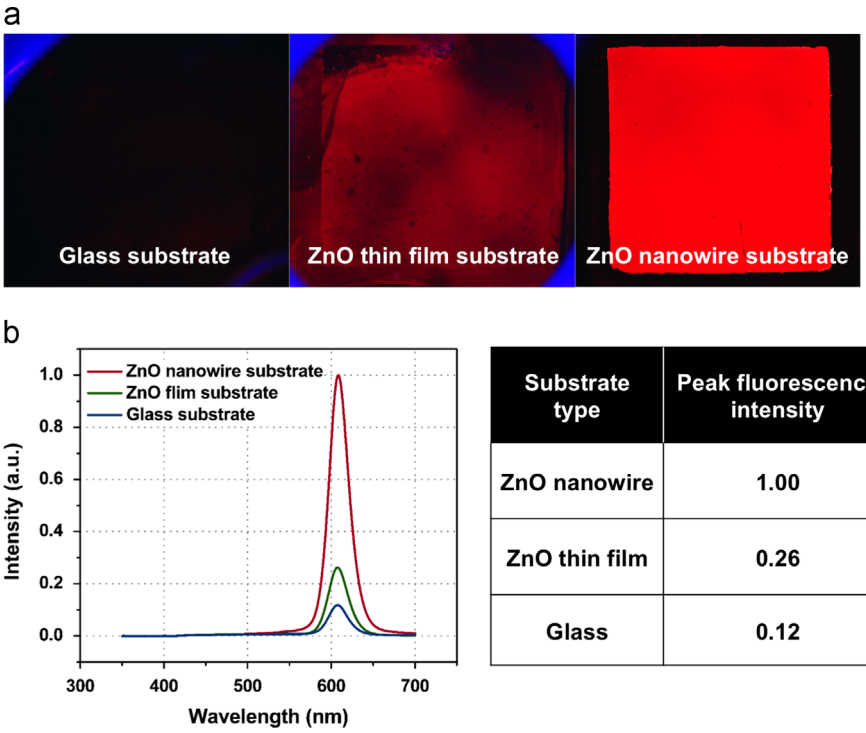

Substrate type	Peak fluorescence intensity
ZnO nanowire	1.00
ZnO thin film	0.26
Glass	0.12

Fig. 3. Effect of biotin–streptavidin complex based anti-FRET layer on the QD fluorescence: (a) fluorescence microscopy images of (left) ZnO nanowire substrate with no anti-FRET layer and (right) ZnO nanowire substrate with triple anti-FRET layers, (b) normalized peak intensity and (λ=605 nm) ,and (c) photospectra of 0, 1, 2, and 3 anti-FRET layers after immunoreaction with QD-conjugated CEA molecules (concentration=10 μg/mL).

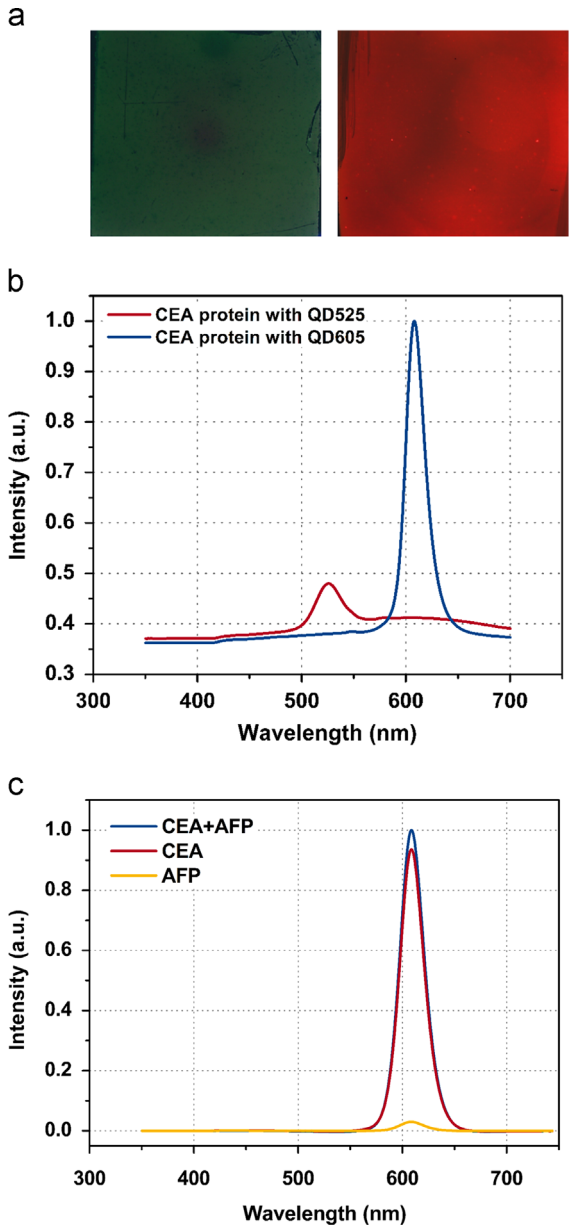

Fig. 4. Fluorescence microscopy image of immunoreaction with CEA proteins (concentration = 10 μg/mL) labeled with (a) (left) QD525 and (right) QD605, (b) spectrum of each QD on ZnO nanowire substrate and (c) photospectra and normalized peak intensity after the immunoreaction with CEA (0.01 mg/mL), AFP (0.01 mg/mL), and CEA and AFP mixture (0.01 mg/mL for both proteins) solution labeling by QD605 conjugated secondary antibody.

method with a mixture solution of CEA and AFP proteins (both at the same concentration of 0.01 mg/mL) in the same platform. As shown in Fig. 4c, the mixture sample of CEA and AFP proteins showed similar fluorescence intensity to that of the pure CEA protein solution (concentration of 0.01 mg/mL). This result proves that the detection signal of the CEA undergoes little interference from other nonspecific proteins. Furthermore, the fluorescence signal to the pure AFP protein (i.e. nonspecific molecules) solution was much smaller (< 2.9%) than that for the pure CEA protein (i.e. target molecules) solution.

Also, we have examined the possibility of nonspecific binding such as direct binding of secondary antibodies to the biotin–streptavidin complex or to the surface of ZnO nanowires by measuring the fluorescence signal from the nonspecific binding (See Fig. S4). The fluorescence signal from the nonspecific binding was less than 10% of that from the specific binding. This result verifies that the effect of nonspecific binding is negligible.

3.3. Fluorescence response from immunoreaction on different substrates

As mentioned earlier, large surface area for immunoreaction is the main advantage of the nanowire substrate. Synthesized ZnO nanowires possess high aspect ratios of 70–100 as shown in Fig. 2a and thus have huge area for surface reaction with analytes. To confirm the large surface reaction area of ZnO nanowires and their advantages for immunoassay, we conducted an immunoreaction of CEA analytes on three different substrates: (a) glass substrate, (b) ZnO thin film substrate, and (c) ZnO nanowire substrate. Here, all examined substrates were modified with three layers of biotin–streptavidin complex. Fig. 5a shows the fluorescence microscopy images from each substrate after immunoreaction. The QD fluorescence exhibited the highest intensity on the ZnO nanowire substrate while almost no light was emitted from the glass substrate. Although the ZnO thin film substrate showed moderate level of fluorescence, its intensity was much lower than that from the ZnO nanowire substrate. Also, clear square patterns of QD fluorescence were observed on the ZnO nanowire substrate, which confirms a significant difference of immunoreactions on the ZnO nanowire substrate and on the glass substrate. The spectrometer measurement data in Fig. 5b also verifies high efficiency of immunoreaction and QD fluorescence on the ZnO nanowire substrate. Regardless of the substrate types, the fluorescence spectrum from each substrate shows the same peak at $\lambda = 605$ nm, which corresponds to the peak wavelength of the QD. However, the ZnO nanowire substrate exhibited 8.5 and 3.8 times higher intensity than that of glass and ZnO thin film substrates, respectively.

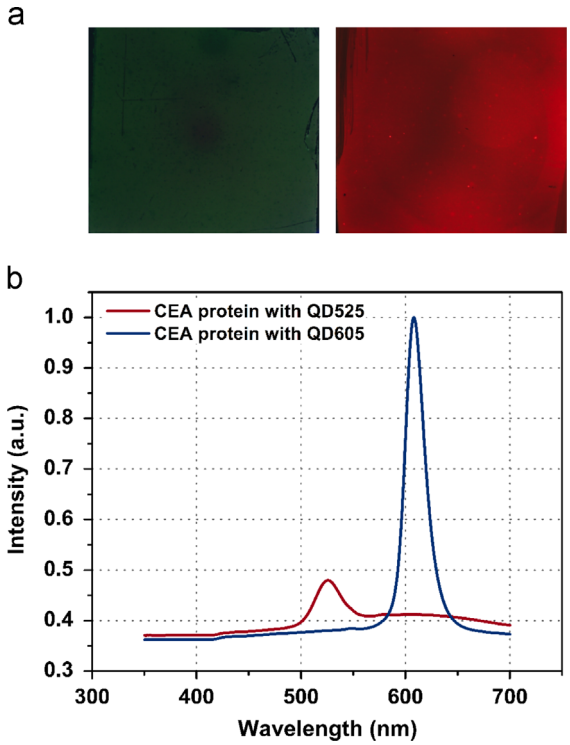

Fig. 5. (a) Fluorescence microscopy images of CEA immunoreaction. (b) Photospectra and normalized peak intensity of QD conjugated CEA on different substrates (glass, ZnO thin film, and ZnO nanowire substrates) after the immunoreaction of QD-conjugated CEA molecules (concentration = 10 μg/mL).

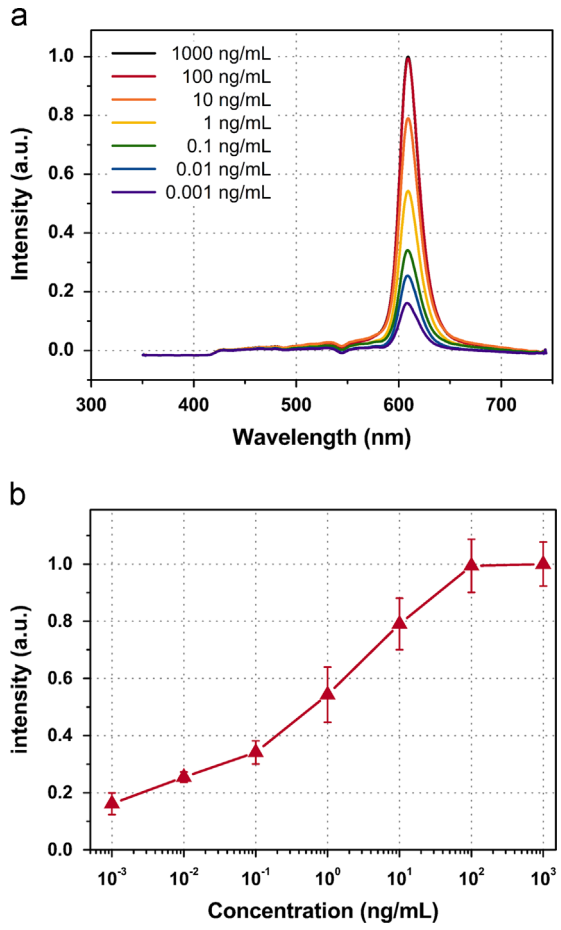

Fig. 6. CEA protein immunoassay at different concentrations on ZnO nanowire substrate from 0.001 ng/mL to 1000 ng/mL. (a) The spectrum of each concentration and (b) peak fluorescence intensity at different concentrations at $\lambda = 605$ nm.

3.4. Effect of protein concentration

To examine the applicability of ZnO nanowire substrate with QD labeling for immunoassay, we quantified the concentration of CEA protein, which is a well-known biomarker for various types of cancers. The CEA protein diluted in PBS solution with concentrations from 0.001 ng/mL to 1000 ng/mL (i.e. from 5 fM to 5 nM) was introduced on the ZnO nanowire substrate decorated with triple layers of anti-FRET biotin–streptavidin complex and monoclonal Ab. The fluorescence spectra at different CEA concentrations are shown in Fig. 6a. Each spectrum showed the same peak wavelength at $\lambda = 605$ nm while the fluorescence intensity was increased for higher CEA concentration. The normalized peak intensity vs. CEA concentration is plotted in Fig. 6b. In the concentration range of 0.1–100 ng/mL, the fluorescence intensity is logarithmically proportional to the CEA concentration. The limit of detection appears to be lower than 0.001 ng/mL and saturation occurs above 100 ng/mL.

CEA antigen has been detected as a cancer biomarker for the diagnosis of various cancers, including gastric cancer (He et al., 2013), pancreatic cancer (Wang, 2009), lung cancer (Okamura et al., 2013), etc. In the case of gastric cancer, optimum positive boundary value of CEA is known to be 2.24 ng/mL. Different boundary values are used for different cancer types but typical range for cancer marker detection is in the range of a few to few tens of nanograms per milliliter (He et al., 2013). Our QD labeling immunoassay on ZnO nanowire substrate can perform as an excellent cancer diagnostic immunosensor for CEA molecules in the clinically meaningful concentration range. Table S1 (in the Supporting information) shows the detection limit and dynamic range of previously reported immunoassay methods (Guo et al., 2013; Hu et al., 2013; Liu et al., 2013; Sun et al., 2013; Tian et al., 2012). As compared to previously developed methods, our approach can provide both low detection limit (< 1 pg/mL) and large dynamic range (1 pg/mL–100 ng/mL) at the same time. In electrochemical or electrochemiluminescence immunoassays, they show lower limit of detection which is around a few pg/mL or even down to a few fg/mL (Guo et al., 2013; Liu and Ma, 2013). However, they have much narrower detection ranges for CEA such as 0.001–0.1 pg/mL, which does not cover the whole working range for CEA as a cancer biomarker. In contrast, the immunoassay platform developed in this work has enabled a very wide detection range (from 0.001 ng/mL to 100 ng/mL).

4. Conclusion

In this work, we introduced a new concept of immunoassay platform based on quantum dots and nanowires for the development of ultra-sensitive and high performance immunoassay. ZnO nanowire was utilized as an efficient substrate for analyte detection with QD labeling. The high surface to volume ratio of ZnO nanowires facilitates a large surface area for immunoreaction with stronger fluorescence signal than conventional glass-based immunoassay substrates. We observed FRET phenomenon from the QDs to the ZnO nanowires, which hinders the fluorescence signal from the QDs. However, we could efficiently suppress the FRET phenomenon and preserve the original fluorescence properties of QDs on the surface of ZnO nanowires by applying the anti-FRET layer based on biotin–streptavidin complex. The FRET phenomenon could be suppressed by controlling the number of anti-FRET layers. We have verified that ZnO nanowire substrate provides an outstanding performance for the immunoassay over conventional substrates due to the large surface area for immunoreaction. ZnO nanowire substrate exhibited much higher intensity than that of planar substrates for the same analyte concentration. Also, we demonstrated the immunoassay of CEA antigen on the ZnO nanowire substrate with quantum dots. This immunoassay platform based on QD labeled nanowire substrate has two main advantages; 1) high sensing performance with wide detection range (0.001–100 ng/mL) and low detection limit (0.001 ng/mL) by utilizing large reaction surface area of vertical nanowire array and 2) potential applicability of various types of QD materials for multiplexed immunoassay with good selectivity. With these advantages over conventional immunoassay tools, this platform can be used for the detection of a wide range of biomarker proteins in cancer cells for the personalized cancer diagnosis at a molecular level. We believe that our novel platform can provide a convenient and highly efficient sensing technology for a variety of biomolecules.

Acknowledgments

This research was supported by a National Leading Research Laboratory Program (Grant NRF-2013R1A2A1A05006378), Global Frontier Project (CISS-2012M3A6A6054201) and Global Ph.D. Fellowship (2012057022) through the National Research Foundation funded by the Ministry of Science, ICT and Future Planning of Korea.

Appendix A. Supplementary material

Supplementary data associated with this article can be found in the online version at http://dx.doi.org/10.1016/j.bios.2013.12.007.

References

Chang, J.Y., Kim, T.G., Sung, Y.M., 2011. Nanotechnology 22 (42), 425708.
Chen, J., Li, C., Zhao, D., Lei, W., Zhang, Y., Cole, M., Chu, D., Wang, B., Cui, Y., Sun, X., 2010. Electrochem. Commun. 12 (10), 1432–1435.
Dorfman, A., Kumar, N., Hahm, J., 2006a. Adv. Mater. 18 (20), 2685–2690.
Dorfman, A., Kumar, N., Hahm, J.I., 2006b. Langmuir 22 (11), 4890–4895.
Greene, L.E., Yuhas, B.D., Law, M., Zitoun, D., Yang, P.D., 2006. Inorg. Chem. 45 (19), 7535–7543.
Guo, Z.Y., Hao, T.T., Du, S.P., Chen, B.B., Wang, Z.B., Li, X., Wang, S., 2013. Biosens. Bioelectron. 44, 101–107.
He, C.Z., Zhang, K.H., Li, Q., Liu, X.H., Hong, Y., Lv, N.H., 2013. BMC Gastroenterol.13.
He, Y., Zhong, Y.L., Su, Y.Y., Lu, Y.M., Jiang, Z.Y., Peng, F., Xu, T.T., Su, S., Huang, Q., Fan, C.H., Lee, S.T., 2011. Angew. Chem. Int. Ed. 50 (25), 5694–5697.
Hu, M., Yan, J., He, Y., Lu, H.T., Weng, L.X., Song, S.P., Fan, C.H., Wang, L.H., 2010. Am. Chem. Soc. Nano 4 (1), 488–494.
Hu, W.H., Lu, Z.S., Liu, Y.S., Chen, T., Zhou, X.Q., Li, C.M., 2013. Lab Chip 13 (9), 1797–1802.
Kumar, C.S.S.R., 2007. Nanomaterials for Biosensors. Wiley-VCH, Weinheim.
Leschkies, K.S., Divakar, R., Basu, J., Enache-Pommer, E., Boercker, J.E., Carter, C.B., Kortshagen, U.R., Norris, D.J., Aydil, E.S., 2007. Nano Lett. 7 (6), 1793–1798.
Liu, H.G., Zhang, X.F., Xing, B.G., Han, P.Z., Gambhir, S.S., Cheng, Z., 2010a. Small 6 (10), 1087–1091.
Liu, J., Lau, S.K., Varma, V.A., Moffitt, R.A., Caldwell, M., Liu, T., Young, A.N., Petros, J.A., Osunkoya, A.O., Krogstad, T., Leyland-Jones, B., Wang, M.D., Nie, S.M., 2010b. Am. Chem. Soc. Nano 4 (5), 2755–2765.
Liu, Z.M., Ma, Z.F., 2013. Biosens. Bioelectron. 46, 1–7.
Medintz, I.L., Clapp, A.R., Mattoussi, H., Goldman, E.R., Fisher, B., Mauro, J.M., 2003. Nat. Mater. 2 (9), 630–638.
Okamura, K., Takayama, K., Izumi, M., Harada, T., Furuyama, K., Nakanishi, Y., 2013. Lung Cancer 80 (1), 45–49.
Peng, W.B., He, Y.N., Wen, C.B., Ma, K., 2012. Sens. Actuators A—Phys. 184, 34–40.
Sun, G.Q., Lu, J.J., Ge, S.G., Song, X.R., Yu, J.H., Yan, M., Huang, J.D., 2013. Anal. Chim. Acta 775, 85–92.
Tak, Y.K., Naoghare, P.K., Kim, B.J., Kim, M.J., Lee, E.S., Song, J.M., 2012. Nano Today 7 (4), 231–244.
Tian, J.N., Zhou, L.J., Zhao, Y.C., Wang, Y., Peng, Y., Hong, X., Zhao, S.L., 2012. J. Fluoresc. 22 (6), 1571–1579.
Wang, L.Y., Wang, J., Zhang, S.L., Sun, Y., Zhu, X.N., Cao, Y.B., Wang, X.H., Zhang, H.Q., Song, D.Q., 2009. Anal. Chim. Acta 653 (1), 109–115.
Wang, Z.L., 2009. Mater. Sci. Eng. R—Rep. 64 (3–4), 33–71.
Zheng, G.F., Patolsky, F., Cui, Y., Wang, W.U., Lieber, C.M., 2005. Nat. Biotechnol. 23 (10), 1294–1301.
Zrazhevskiy, P., Gao, X.H., 2013. Nat. Commun. 4, 1619.